RSC Advances

ROYAL SOCIETY OF CHEMISTRY

www.rsc.org/advances

Synthesis, molecular modeling, and biological evaluation of quinazoline derivatives containing 1,3,4-oxadiazole scaffold as novel inhibitors of VEGFR2

Fang Qiao [b +], *Yong Yin* [b +], *Yu-Ning Shen* [b], *She-Feng Wang* [b], *Shao Sha* [b], *Xun Wu* [b], *Ai-Min Lu* [c], *Chen Xu* [b *], *Wei-Ming Zhang* [a *], *Hai-Liang Zhu* [b *]

[a] *Nanjing Institute for the Comprehensive Utilization of Wild Plant, Nanjing 210042, People's Republic of China*

[b] *State Key Laboratory of Pharmaceutical Biotechnology, Nanjing University, Nanjing 210093, People's Republic of China*

[c] *College of Science, Nanjing Agriculture University, Nanjing 210095, People's Republic of China*

[+] *These authors contributed equally to this work.*

[*] *Corresponding authors. Tel.: +86 25 83592572; Fax: +86 25 83592672.*

E-mail address: botanyzh@163.com (W.-M. Zhang), zhuhl@nju.edu.cn_x000D_(H.-L. Zhu).

Abstract

A series of 4-alkoxyquinazoline derivatives containing 1,3,4-oxadiazole scaffold have been designed and synthesized, and their inhibitory activities were also tested against A549, MCF-7 and Hela. Of these compounds, 2-(3,4-Dimethoxybenzyl)-5-((quinazolin-4-yloxy)methyl)-1,3,4-oxadiazole(compound **4j)** showed the most potent inhibitory activity (IC_{50} = 0.23 μM for MCF-7, IC_{50}= 0.38 μM for A549 and IC_{50} = 0.32 μM for Hela) and the effect was better than the positive control drug Tivozanib (IC_{50} = 0.38 μM for MCF-7, IC_{50}= 0.62 μM for A549 and IC_{50} = 0.34 μM for Hela). Docking simulation was performed to position compound **4j** into the VEGFR active site to determine the probable binding model. These results suggested that compound **4j** with potent inhibitory activity in tumor growth inhibition may be a potential anticancer agent.

Keywords:

Quinazoline

1,3,4-oxdiazole

VEGFR2

Anticancer

1. Introduction

The malignant tumor is currently the first murderer which threaten the human's health and life in the world.[1,2] So anti-cancer is then taken all important task by WHO and Health Department of countries.[3] Although several classes of anti-cancer agents are presently available, severer side-effect and drug resistance constantly emerges.[4] Therefore, the elaboration of new types of anticancer drugs is a critical task that can prevent this serious medical problem. Recently, different targets in key steps of the growth and proliferation of cancer cell have been studied that could be a new weapon against tumor.[5]

Tumour cell growth or hyperplasia is a fairly complex process, and involves a series of steps.[6] Angiogenesis, which is the formation of new blood vessels , is not only a pivotal step during the formation of metastases but also the focus of researchers all over the world.[7] Vascular endothelial growth factor (VEGF) play a significant role in tumor angiogenesis, vascular permeability, endothelial cell activation, proliferation, and migtation.[8] The VEGF family consists of VEGF-A, VEGF-B, VEGF-C,VEGF-D, and placenta growth factor (PlGF).[9] The biological functions of VEGF are achieved through the interaction with the VEGF receptor family. In mammals, the VEGFR family is transmembrane tyrosine kinases and consists of three members, VEGFR1, VEGFR2 and VEGFR3.[10] The VEGFRs consist of three parts: an extracellular ligand-binding domain, an intracellular tyrosine kinase domain and a single transmembrane segment.[11,12] Binding of VEGF to VEGFR results in receptor dimerization, which leads to phosphorylation and dimerization on downstream signal transducer proteins.[10,11] This VEGFR tyrosine kinase-mediated cell growth signaling pathway is an important signaling pathway in role in regulating the proliferation of many types of tumors, such as breast cancer,[13] non small cell lung cancer,[14] head and neck cancer,[15] glioblastomas.[16] VEGFR2 plays major a role in regulation of VEGF-driven responses in endothelial cells and it is proven to be a prerequisite signal transducer in tumorgenesis.[17] Therefore, VEGFR2 might be the hottest target in current research. In recent years, a number of compounds have been reported as

potent inhibitors of VEGFR2 in vitro or possessed antiangiogenic activity (Figure 1), such as Vandetanib,[18] Sorafenib (BAY-43-9006),[19] Tivozanib,[20] ZD4190.[21]

As shown in Figure 1, the scaffolds of the known inhibitors of VEGFR2 can be divided into two main groups: those contain a core of 4-anilino-quinazoline; others contain a core of 4-ol-quinoline. Given the above information our group have designed and synthesized a series of new compounds by employed a similar template with scaffold 4-ol-quinzoline core,[22] with the presumption that the quinazoline core can be a common scaffold of VEGFR2 inhibitors which inhibits VEGFR2 by binding to the kinase domain via the gatekeeper Cys919 and Phe918 of VEGFR2.[23,24] The results showed that compound S1(4-(2-(2-methyl-5-nitro-1H-imidazol-1-yl)ethoxy) quinazoline) has obviously inhibitory activities against VEGFR2 (Figure 1), the IC_{50} value of S1 was 0.43 μM for MCF-7.

Besides, 1,3,4-oxadiazole is a heterocyclic structure matrix with extensive biological activity.[25,26] In particular, a few 2,5-disubstituted 1,3,4-oxadiazole have been found with some extent of anticancer activities.[27,28] Furthermore, as the special structure of 1,3,4-oxadiazole heterocycles: good bioisosteres of amides and esters, they can improve the pharmacological activity via hydrogen bonding interactions with the receptors.[20,30]

Considering the above mentioned facts, on the basis of our proceeding work, we designed and synthesized a series of new 4-alkoxyquinazoline derivatives containing 1,3,4-oxadiazole moiety and studied their antitumor activities against A549, MCF-7 and Hela cell lines, respectively. The interactions of these quinazoline-based analogs with the ATP binding site of VEGFR2 (PDB code: 4ASE) were studied via molecular docking.

2. Results and discussion

2.1. Chemistry

Compound **3** was synthesized by the routes outlined in Scheme 1 according to Mirzaei et al.'s method.[31] Compound **3** was prepared by the reaction of

4-Hydroxyquinazolinein excess ethyl-bromacetateand then hydrazinolysis of ethyl ester group by hydrazine hydrate with yield of 78%.

2-(Quinazolin-4-yloxy)acetohydrazide was then reacted with substituted benzoic acids and phenylacetic acids to prepare the corresponding quinozoline derivatives **4a-4v**. The chemical structures of these quinozoline derivatives were displayed in Table 1. All these compounds gave satisfactory elementary analyses (±0.4%). ^{1}H NMR and ESI MS spectra data was consistent with the assigned structures.

2.2. Biological activity

2.2.1. Antiproliferative effects against cancer cells

The target compounds were evaluated by in vitro anti-proliferation assays against three human cancer cell lines A549, MCF-7 (with VEGFR protein over expression) and Hela to test the antitumour activities of the synthesized compounds. The results are indicated in Table 2. Most compounds showed a remarkable potent antitumor activity, indicating that 4-alkoxyquinazoline derivatives containing 1,3,4-oxadiazole scaffold could possess a significant anticancer potency. Among these compounds, it was observed that **4j** showed the most potent biological activity (IC_{50} = 0.23 μM for MCF-7), comparable to the positive control tivozanib (IC_{50} = 0.38 μM for MCF-7).

From the data listed in Table 2, we could draw the conclusion that the activity of the tested compounds may be correlated to the variation and modifications of the structure. Among the 22 synthetic new 4-alkoxyquinazoline derivatives, the phenylacetic acid derivatives **4a-4k**, whose IC_{50} values ranging from 0.23 to 16.23 μM displayed higher antitumor potencies than benzoic acid derivatives **4l-4v**, with IC_{50} values ranging from 6.32 to 54.35 μM, which demonstrate the introduction of phenylacetic acid resulted in the decline of anticancer activity. Such as p- position nitro group, compound **4d** with benzyl group exhibited superior activity compared with compound **4v** which with phenyl group. This conclusion that the long carbon chain increased the anticancer activity of quinazoline derivatives can provide a significant contribution to design the effective length of carbon chain of the quinazoline derivative with best antitumor activity. Moreover, among the eleven

quinazoline derivatives (**4a-4k**), compound **4j** showed most potent activities with IC_{50} value of 0.23 μM against MCF-7 (breast cancer), which is superior to the positive control tivozanib with corresponding IC_{50} value of 0.38 μM. In addition, the data showed compound **4j** displayed significant activities with IC_{50} value of 0.32, 0.38 μM against A549 and Hela, respectively, indicating that they possessed potent anticancer activities. And the varieties of substitutes of phenylacetic acid such as halogen, nitryl and methoxyl also lead to the different anticancer activities. Among them, we can observed that compounds with electron-donating substituents (such as OCH_3) improved the VEGFR2 inhibitory activity compared to those with halogen substituents (such as F, Cl, Br). In addition, a comparision of the p- position on phenylacetic acid demonstrated that p- position halogen group (**4e, 4c, 4g**) improved VEGFR2 inhibitory activity and the potency order is F < Cl < Br and we found the same law for the p- position on benzoic acid (**4q, 4s, 4t**). Other p- position substitutions such as **4p** with a methyl group substitutent have slightly improved the activity. Last but not least, compounds with the same group on the o-, m- and p- position lead to different activity. We found that derivatives with a methoxy group on the m- position and p- position of phenylacetic acid of displayed higher antitumor activity with IC_{50} value of 0.87, 0.77 μM against MCF-7 than compound with a methoxy group on the o- position of phenylacetic acid with IC_{50} value of 1.64 μM against MCF-7. Given the suggestions, we designed and evaluated the compound with 3,4-dimethoxy group substitution (**4j**), the activity was significantly enhanced up to 0.23 μM against MCF-7.

2.2.2. Kinase selectivity

In order to validate the anti-proliferative effect was produced by interaction of VEGFR protein and synthesized compounds, all compounds of the series were subjected to in vitro VEGFR2, EGFR (epidermal growth factor receptor), bFGF (basic fibroblast growth factor) and PDGFR (platelet-derived growth factor receptor) kinase inhibitory assays. As shown in Table 3, all synthesized compounds showed much more higher inhibitory activity for VEGFR2 than for EGFR, bFGF and PDGFR,

like reference Tivozanib. Additionally, good agreement was found between the IC_{50} values of these compounds and their relevant IC_{50} values in the anti-proliferative assay. Hence, a further study comparing the anti-proliferative activity against the MCF-7 cell line with the VEGFR2 inhibitory activity of the top 10 compounds (**4j, 4d, 4f, 4b, 4g, 4a, 4h, 4c, 4l, 4e**) was performed and the result revealed that there was a moderate correlation between VEGFR2 inhibition and the inhibition of cancer cellular proliferation, as evidenced in Figure 2, with a correlation coefficient of 7.4071 and an R^2 value of 0.9345. In conclusion, the synthesized compounds can inhibit the function of VEGFR2 and the anti-proliferative effect was produced partly by interaction of VEGFR2 protein and the molecule inhibitors.

2.2.3. Molecular docking

In order to gain more understanding of the structure-activity relationships observed at the VEGFR2, molecular docking of the most potent inhibitor **4j** and the positive compound Tivozanib into the active site of the VEGFR2 complex structure (PDB code: 4ASE).[32]

All docking runs were applied LigandFit Dock protocol of Discovery Studio 3.5. The CDOCKER_INTERACTION_ENERGY of the synthesized compounds was showed in Table 4. The CDOCKER_INTERACTION_ENERGY of the synthesized compounds demonstrated that these compounds have good affinity to the active site of 4ASE, which further proved the positive correlation between the CDOCKER_INTERACTION_ENERGY and their anticancer activity. Among the docking calculation of the synthesized compounds, compound **4j** showed the lowest interaction energy -50.5831 kcal/mol (Table 4). The binding model of compound **4j** and VEGFR2 is depicted in Figure 3 and Figure 4. Figure 3 and Figure 4 showed the binding mode of compound **4j** interacting with VEGFR2 protein and the docking results revealed that four amino acids Lys868, Cys919, His1026 and Asp1046 located in the binding pocket of the protein played vital roles in the conformation with compound **4j**, which were stabilized by three π-π bonds and two hydrogen bonds that are shown in the 2D and 3D diagrams. Two π-π interactions were formed between

His1026 and the quinazoline ring with 4.87682 Å and 6.00074 Å while the other π-π interaction bond with 5.05787 Å involved Lys868. One hydrogen bond with 2.5 Å was formed between Cys919 and the phenylacetic acid ring. Another one hydrogen bond was formed between Asp1046 and **4j**. Figure 5 and Figure 6 showed the interaction of the positive compound Tivozanib and the 4ASE. From the two pictures, we can draw a conclusion that two amino acid residues Cys919 and Asp1046 located in the binding pocket of 4ASE played a key role in the conformation. As illustrated in Figure 4 and Figure 6, there was a hydrogen bond between the hydrogen of quinazoline ring of Tivozanib and the oxygen of carboxyl group of Cys919, while a hydrogen bond between oxygen of methoxy group of compound **4j** and the hydrogen of amino group of Cys919. The Figures also suggested that compound **4j** and Tivozanib appeared to be interact with the hydrogen of amino group of Asp1046 through hydrogen bonds. The docking results of Tivozanib and 4ASE revealed that compound **4j** had a high binding affinities of 4ASE. In addition, there were three π-π stacking interactions between quinazoline ring and the benzene ring of Lys868, His1026. The π-π interaction energies are of the same order of magnitude as hydrogen bonds and make the complex more stable. Therefore, compound **4j** showed the interaction energy -50.5831 kcal/mol lower than the -47.6633 kcal/mol of Tivozanib.The enzyme assay data and the molecular docking results demonstrated that compound **4j** was a potential inhibitor of VEGFR2.

3. Conclusion

To sum up, a series of 4-alkoxyquinazoline derivatives containing 1,3,4-oxadiazole scaffold have been designed and synthesized, and their inhibitory activities were also tested against A549, MCF-7 and Hela cell lines. Compound **4j** exhibited the most potent inhibitory activity (IC_{50} = 0.23 μM for MCF-7, IC_{50}= 0.38 μM for A549 and IC_{50} = 0.32 μM for Hela), which was compared with the positive control tivozanib. Preliminary SARs and molecular modeling study provided further insight into interactions between the enzyme and its ligand. Analysis of the compound **4j**'s binding conformation in active site displayed the compound **4j** was stabilized by

the interactions with Lys868, Cys919, His1026 and Asp1026. The result provided valuable information for the design of VEGFR2 inhibitors as antitumor agents.

4. Experiments

4.1. Materials and measurements

All chemicals (reagent grade) used were commercially available. All of the synthesized compounds were chemically characterized by thin layer chromatography (TLC), proton nuclear magnetic resonance (1H NMR) and elemental microanalyses (CHN). Analytic thin-layer chromatography (TLC) was performed on the glass-backed silica gel sheets (silica gel 200 Å GF254). All compounds were detected using UV light (254 nm or 365 nm). Melting points were determined using an XT4 MP apparatus (Taike Corp, Beijing, China) and are as read. 1H NMR spectra were measured using a Bruker AV-400 spectrometer at 25 □ and referenced to Me4Si. Chemical shifts are reported in ppm (δ) using the residual solvent line as an internal standard. ESI-MS spectra were recorded using a Mariner System 5304 mass spectrometer. Elemental analyses were performed using a CHN-O-Rapid instrument and were within ± 0.4% of the theoretical values.

4.2. Chemistry

4.2.1. General procedure for synthesis of compound 2.

A mixture of 4-hydroxyquinazoline (0.01 mol), ethyl-bromacetate (0.015 mol), Cs_2CO_3 (0.02 mol) was dissolved in 30 mL DMF on 80 □ for 24 h. The mixture was poured into water. The products were extracted with ethyl acetate. The extract was dried over anhydrous Na_2SO_4, filtered and evaporated to give compound **2**.

4.2.2. General procedure for synthesis of compound 3.

To a stirring solution of hydrazine hydrate (6.5 mL) in an ice bath, a solution of compound **2** (0.03 mol) in methanol (40 mL) was added slowly (10 min). The stirring was continued for 4.5 h at 0 □ under argon atmosphere. The white precipitate which formed in -10 □ was filtered and recrystallized from chloroform to give compound **3**.

4.2.3. General procedure for synthesis of compound 4a-4v.

An equimolar mixture of compound **3** (0.001 mol) and substituted carboxylic acids (0.001 mol) in phosphoryl chloride (15 mL) was refluxed for 10-16 h. Then reaction mixture was cooled, poured into ice-cold water and neutralized with 20% $NaHCO_3$ solution. The resultant solid was filtered, washed with water and recrystallized from ethanol to give 1,3,4-oxadiazole derivatives **4a-4v**.

4.2.3.1. 2-(3-Bromobenzyl)-5-((quinazolin-4-yloxy)methyl)-1,3,4-oxadiazole (4a)

Yield: 59%; m.p. 116-118 □. ^{1}H NMR(400 MHz, DMSO): 4.27(s, 2H), 5.45(s, 2H), 7.27(d, *J*=8.32 Hz, 2H), 7.57(m, 3H), 7.73(d, *J*=8.08 Hz, 1H), 7.88(m, 1H), 8.14(m, 1H), 8.49(s, 1H). ^{13}C NMR (101 MHz, DMSO) δ: 166.60, 163.24, 160.37, 148.34, 148.06, 140.53, 135.36, 130.28, 128.45, 128.30, 127.99, 127.85, 126.75(2), 124.23, 121.76, 41.15, 30.55. MS (ESI): 398.53 ($C_{18}H_{14}BrN_4O_2$, $[M+H]^+$). Anal.Calcd for $C_{18}H_{13}BrN_4O_2$: C, 54.43; H, 3.30; N, 14.10%. Found: C, 54.45; H, 3.32; N, 14.08%.

4.2.3.2. 2-(3-Methoxybenzyl)-5-((quinazolin-4-yloxy)methyl)-1,3,4-oxadiazole (4b)

Yield: 53%; m.p. 197-199 □. ^{1}H NMR(400 MHz, DMSO): 3.71(s, 3H), 4.23(s, 2H), 5.46(s, 2H), 6.84(d, *J*=7.88 Hz, 3H), 7.24(t, *J*=7.52 Hz, 1H), 7.59(m, 1H), 7.73(d, *J*=7.92 Hz, 1H), 7.88(m, 1H), 8.14(m, 1H), 8.50(s, 1H). ^{13}C NMR (101 MHz, DMSO) δ: 169.11, 166.18, 160.58, 159.61, 148.95, 148.49, 137.54, 134.97, 129.69, 127.71, 127.60, 126.44, 121.68(2), 115.15, 112.37, 55.39, 41.19, 30.79. MS (ESI): 349.39 ($C_{19}H_{17}N_4O_3$, $[M+H]^+$). Anal.Calcd for $C_{19}H_{16}N_4O_3$: C, 65.51; H, 4.63; N, 16.08%. Found: C, 65.53; H, 4.61; N, 16.11%.

4.2.3.3. 2-(4-Chlorobenzyl)-5-((quinazolin-4-yloxy)methyl)-1,3,4-oxadiazole (4c)

Yield: 48%; m.p. 248-251 □. ^{1}H NMR(400 MHz, DMSO): 4.28(s, 2H), 5.46(s, 2H), 7.33(m, 2H), 7.39(d, *J*=8.48 Hz, 2H), 7.58(m, 1H), 7.72(d, *J*=8.12 Hz, 1H),

7.87(m, 1H), 8.14(m, 1H), 8.50(s, 1H). ^{13}C NMR (101 MHz, DMSO) δ: 168.38, 163.51, 160.36, 150.58, 148.04, 134.33(2), 130.85(2), 128.01, 127.85, 127.25(2), 126.57, 123.11, 121.76, 41.12, 30.57. MS (ESI): 353.23 ($C_{18}H_{14}ClN_4O_2$, $[M+H]^+$). Anal.Calcd for $C_{18}H_{13}ClN_4O_2$: C, 61.28; H, 3.71; N, 15.88%. Found: C, 61.25; H, 3.72; N, 15.86%.

4.2.3.4. 2-(4-Nitrobenzyl)-5-((quinazolin-4-yloxy)methyl)-1,3,4-oxadiazole (4d)

Yield: 40%; m.p. 129-130 □. ^{1}H NMR(400 MHz, DMSO): 4.47(s, 2H), 5.47(s, 2H), 7.58(m, 3H), 7.72(d, *J*=8.50 Hz, 1H), 7.87(m, 1H), 8.14(m, 1H), 8.20(d, *J*=8.76 Hz, 2H), 8.50(s, 1H). ^{13}C NMR (101 MHz, DMSO) δ: 165.58, 163.28, 160.37, 148.26, 148.07, 147.23, 142.56, 135.35, 130.88(2), 127.99, 127.85, 126.57(2), 124.21, 121.76, 41.12, 30.70. MS (ESI): 364.83 ($C_{18}H_{14}N_5O_4$, $[M+H]^+$). Anal.Calcd for $C_{18}H_{13}N_5O_4$: C, 59.50; H, 3.61; N, 19.28%. Found: C, 59.51; H, 3.63; N, 19.31%.

4.2.3.5. 2-(4-Fluorobenzyl)-5-((quinazolin-4-yloxy)methyl)-1,3,4-oxadiazole (4e)

Yield: 53%; m.p. 109-110 □. ^{1}H NMR(400 MHz, DMSO): 4.27(s, 2H), 5.46(s, 2H), 7.16(t, *J*=8.84 Hz, 2H), 7.35(m, 2H), 7.58(t, *J*=7.16 Hz, 1H), 7.73(d, *J*=8.04 Hz, 1H), 7.88(m, 1H), 8.14(m,1H), 8.50(s, 1H). ^{13}C NMR (101 MHz, DMSO) δ: 166.45, 163.22, 160.38, 150.39, 148.91, 148.40, 135.35, 130.57(2), 127.89, 126.93, 126.51, 124.21, 121,74, 113.41(2), 41.13, 30.69. MS (ESI): 337.92 ($C_{18}H_{14}FN_4O_2$, $[M+H]^+$). Anal.Calcd for $C_{18}H_{13}FN_4O_2$: C, 64.28; H, 3.90; N, 16.66%. Found: C, 64.25; H, 3.91; N, 16.68%.

4.2.3.6. 2-(4-Methoxybenzyl)-5-((quinazolin-4-yloxy)methyl)-1,3,4-oxadiazole (4f)

Yield: 62%; m.p. 110-111 □. ^{1}H NMR(400 MHz, DMSO): 3.72(s, 3H), 4.18(s, 2H), 5.45(s, 2H), 6.88(d, *J*=8.64 Hz, 2H), 7.21(d, *J*=8.60 Hz, 2H), 7.58(t, *J*=7.88 Hz, 1H), 7.73(d, *J*=8.04 Hz, 1H), 7.88(m, 1H), 8.15(m, 1H), 8.49(s, 1H). ^{13}C NMR (101 MHz, DMSO) δ: 166.75, 163.03, 160.37, 158.89, 148.27, 148.09, 135.32, 130.44(2), 127.98, 127.84, 126.59, 126.51, 121.77, 114.55(2), 55.53, 41.15, 30.18. MS (ESI): 349.83 ($C_{19}H_{17}N_4O_3$, $[M+H]^+$). Anal.Calcd for $C_{19}H_{16}N_4O_3$: C, 65.51; H, 4.63; N,

16.08%. Found: C, 65.52; H, 4.65; N, 16.11%.

4.2.3.7. 2-(4-Bromobenzyl)-5-((quinazolin-4-yloxy)methyl)-1,3,4-oxadiazole (4g)

Yield: 54%; m.p. 115-117 □. ^{1}H NMR(400 MHz, DMSO): 4.26(s, 2H), 5.45(s, 2H), 7.27(d, *J*=8.44 Hz, 2H), 7.57(m, 3H), 7.73(d, *J*=7.96 Hz, 1H), 7.88(m, 1H), 8.14(m, 1H), 8.49(s, 1H). ^{13}C NMR (101 MHz, DMSO) δ: 166.09, 163.16, 160.37, 148.27, 135.34, 134.19, 132.03(2), 131,68(2), 127.99, 127.86, 126.59, 121.77, 120.97, 41.39, 30.36. MS (ESI): 398.98 ($C_{18}H_{14}BrN_4O_2$, $[M+H]^+$). Anal.Calcd for $C_{18}H_{13}BrN_4O_2$: C, 54.43; H, 3.30; N, 14.10%. Found: C, 54.40; H, 3.32; N, 14.11%.

4.2.3.8. 2-(2-Methoxybenzyl)-5-((quinazolin-4-yloxy)methyl)-1,3,4-oxadiazole (4h)

Yield: 48%; m.p. 101-102 □. ^{1}H NMR(400 MHz, DMSO): 3.70(s, 3H), 4.15(s, 2H), 5.44(s, 2H), 6.91(t, *J*=7.40 Hz, 1H), 6.99(d, *J*=8.16 Hz, 1H), 7.26(m, 2H), 7.59(t, *J*=7.16 Hz, 1H), 7.73(d, *J*=7.96 Hz, 1H), 7.88(m, 1H), 8.14(m, 1H), 8.50(s, 1H). ^{13}C NMR (101 MHz, DMSO) δ: 166.35, 162.76, 160.35, 157.45, 148.19(2), 135.34, 130.84, 129.45, 128.00, 127.85, 126.57, 122.60(2), 120.92, 111.54, 55.87, 41.15, 30.06. MS (ESI): 349.79 ($C_{19}H_{17}N_4O_3$, $[M+H]^+$). Anal.Calcd for $C_{19}H_{16}N_4O_3$: C, 65.51; H, 4.63; N, 16.08%. Found: C, 65.50; H, 4.62; N, 16.05%.

4.2.3.9. 2-Benzyl-5-((quinazolin-4-yloxy)methyl)-1,3,4-oxadiazole (4i)

Yield: 56%; m.p. 108-109 □. ^{1}H NMR(400 MHz, DMSO): 4.26(s, 2H), 5.46(s, 2H), 7.30(m, 5H), 7.58(m, 1H), 7.73(d, *J*=7.92 Hz, 1H), 7.88(m, 1H), 8.15(m, 1H), 8.50(s, 1H). ^{13}C NMR (101 MHz, DMSO) δ: 166.63, 163.08, 160.36, 155.33, 148.21, 135.35, 134.25, 129.98(2), 128.75(2), 127.85, 127.78, 125.76, 124.26, 121.76, 41.13, 30.60. MS (ESI): 319.63 ($C_{18}H_{15}N_4O_2$, $[M+H]^+$). Anal.Calcd for $C_{18}H_{14}N_4O_2$: C, 67.91; H, 4.43; N, 17.60%. Found: C, 67.93; H, 4.42; N, 17.62%.

4.2.3.10.

2-(3,4-Dimethoxybenzyl)-5-((quinazolin-4-yloxy)methyl)-1,3,4-oxadiazole (4j)

Yield: 57%; m.p. 96-98 □. ^{1}H NMR(400 MHz, DMSO): 3.70(d, *J*=10.48 Hz, 6H), 4.17(s, 2H), 5.45(s, 2H), 6.80(m, 1H), 6.88(d, *J*=8.28 Hz, 2H), 7.59(m, 1H), 7.73(d, *J*=7.96 Hz, 1H), 7.88(m, 1H), 8.14(m, 1H), 8.50(s, 1H). ^{13}C NMR (101 MHz, DMSO) δ: 166.65, 163.04, 160.39, 149.22, 148.46, 148.07, 135.30, 127.96, 126.56(2), 121.77, 121.33, 112.96(2), 112.34, 55.94, 55.81, 41.16, 30.60. MS (ESI): 379.86 ($C_{20}H_{19}N_4O_4$, $[M+H]^+$). Anal.Calcd for $C_{20}H_{18}N_4O_4$: C, 63.48; H, 4.79; N, 14.81%. Found: C, 63.45; H, 4.78; N, 14.79%.

4.2.3.11. 2-(2-Chlorobenzyl)-5-((quinazolin-4-yloxy)methyl)-1,3,4-oxadiazole (4k)

Yield: 46%; m.p. 92-93 □. ^{1}H NMR(400 MHz, DMSO): 4.29(s, 2H), 5.38(s, 2H), 7.26(m, 2H), 7.38(m, 2H), 7.50(m, 1H), 7.64(d, *J*=7.92 Hz, 1H), 7.80(m, 1H), 8.06(m, 1H), 8.42(s, 1H). ^{13}C NMR (101 MHz, DMSO) δ: 166.37, 163.19, 160.35, 156.79, 148.42, 138.13, 135.36, 134.56, 130.85(2), 128.65, 128.01, 127.83, 124.23, 121.69(2), 41.25, 26.37. MS (ESI): 353.45 ($C_{18}H_{14}ClN_4O_2$, $[M+H]^+$). Anal.Calcd for $C_{18}H_{13}ClN_4O_2$: C, 61.28; H, 3.71; N, 15.88%. Found: C, 61.26; H, 3.73; N, 15.90%.

4.2.3.12. 2-(2-Methoxyphenyl)-5-((quinazolin-4-yloxy)methyl)-1,3,4-oxadiazole (4l)

Yield: 67%; m.p. 162-164 □. ^{1}H NMR(400 MHz, DMSO): 3.80(s, 3H), 5.58(s, 2H), 7.11(m, 1H), 7.23(d, *J*=8.40 Hz, 1H), 7.59(m, 2H), 7.77(m, 2H), 7.89(m, 1H), 8.17(m, 1H), 8.57(s, 1H). ^{13}C NMR (101 MHz, DMSO) δ: 164.59, 163.27, 160.35, 156.36, 148.49, 148.15, 135.36, 129.95(2), 127.83, 127.05, 126.52(2), 124.33, 115.65, 112.94, 55.63, 41.15. MS (ESI): 335.93 ($C_{18}H_{15}N_4O_3$, $[M+H]^+$). Anal.Calcd for $C_{18}H_{14}N_4O_3$: C, 64.66; H, 4.22; N, 16.76%. Found: C, 64.64; H, 4.23; N, 16.78%.

4.2.3.13. 2-(3-Chlorophenyl)-5-((quinazolin-4-yloxy)methyl)-1,3,4-oxadiazole (4m)

Yield: 55%; m.p. 101-103 □. ^{1}H NMR(400 MHz, DMSO): 5.59(s, 2H), 7.61(m, 2H), 7.72(m, 2H), 7.93(m, 3H), 8.16(m, 1H), 8.58(s, 1H). ^{13}C NMR (101 MHz, DMSO) δ: 164.81, 163.28, 160.47, 148.30, 148.14, 135.35, 132.49, 132.06, 128.00(2),

127.88(2), 126.62, 125.78, 125.42, 121.83, 41.13. MS (ESI): 339.25 ($C_{17}H_{12}ClN_4O_2$, $[M+H]^+$). Anal.Calcd for $C_{17}H_{11}ClN_4O_2$: C, 60.28; H, 3.27; N, 16.54%. Found: C, 60.25; H, 3.25; N, 16.55%.

4.2.3.14. 2-(3-Bromophenyl)-5-((quinazolin-4-yloxy)methyl)-1,3,4-oxadiazole (4n)

Yield: 53%; m.p. 108-109 □. ^{1}H NMR(400 MHz, DMSO): 5.52(s, 2H), 7.51(m, 2H), 7.68(d, *J*=8.04 Hz, 1H), 7.80(m, 2H), 7.92(d, *J*=7.84 Hz, 1H), 8.05(m, 1H), 8.11(m, 1H), 8.51(s, 1H). ^{13}C NMR (101 MHz, DMSO) δ: 164.36, 163.38, 160.46, 148.96, 148.30, 135.35, 132.23, 130.59, 129.33, 128.00(2), 127.87(2), 126.63, 125.62, 121.83, 41.12. MS (ESI): 384.94 ($C_{17}H_{12}BrN_4O_2$, $[M+H]^+$). Anal.Calcd for $C_{17}H_{11}BrN_4O_2$: C, 53.28; H, 2.89; N, 14.62%. Found: C, 53.30; H, 2.91; N, 14.61%.

4.2.3.15. 2-(3-Fluorophenyl)-5-((quinazolin-4-yloxy)methyl)-1,3,4-oxadiazole (4o)

Yield: 35%; m.p. 117-118 □. ^{1}H NMR(400 MHz, DMSO): 5,52(s, 2H), 7.43(m, 1H), 7.56(m, 2H), 7.69(m, 2H),7.75(d, *J*=7.80 Hz, 1H), 7.81(m, 1H), 8.09(m, 1H), 8.51(s, 1H). ^{13}C NMR (101 MHz, DMSO) δ: 163.95, 163.36, 160.47, 148.31, 148.14, 135.35, 132.45, 128.00(2), 127.88(2), 126.62, 125.54, 123.35, 121.83, 119.37, 41.17. MS (ESI): 323.84 ($C_{17}H_{12}FN_4O_2$, $[M+H]^+$). Anal.Calcd for $C_{17}H_{11}FN_4O_2$: C, 63.35; H, 3.44; N, 17.38%. Found: C, 63.38; H, 3.45; N, 17.40%.

4.2.3.16. 2-((Quinazolin-4-yloxy)methyl)-5-p-tolyl-1,3,4-oxadiazole (4p)

Yield: 47%; m.p. 131-134 □. ^{1}H NMR(400 MHz, DMSO): 2.38(s, 3H), 5.57(s, 2H), 7.40(d, *J*=8.04 Hz, 2H), 7.59(m, 1H), 7.75(d, *J*=7.96 Hz, 1H), 7.87(m, 3H), 8.16(m, 1H), 8.57(s, 1H). ^{13}C NMR (101 MHz, DMSO) δ: 164.39, 163.36, 160.47, 150.13, 148.15, 135.35, 132.39, 127.88, 127.45(2), 126.62, 126.23(2), 121.42, 120.29, 117.74, 41.13, 23.15. MS (ESI): 319.75 ($C_{18}H_{15}N_4O_2$, $[M+H]^+$). Anal.Calcd for $C_{18}H_{14}N_4O_2$: C, 67.91; H, 4.43; N, 17.60%. Found: C, 67.92; H, 4.45; N, 17.63%.

4.2.3.17. 2-(4-Fluorophenyl)-5-((quinazolin-4-yloxy)methyl)-1,3,4-oxadiazole (4q)

Yield: 65%; m.p. 114-116 □. ^{1}H NMR(400 MHz, DMSO): 5.53(s, 2H), 7.40(t,

J=8.88 Hz, 2H), 7.55(m, 1H), 7.70(d, *J*=8.12 Hz, 1H), 7.84(m, 1H), 7.99(m, 2H), 8.12(m, 1H), 8.53(s, 1H). ^{13}C NMR (101 MHz, DMSO) δ: 164.17, 163.40, 160.46, 148.31, 148.14, 135.35, 129.84, 129.75, 128.00(2), 127.88(2), 126.62, 121.83, 117.31, 117.14, 41.15. MS (ESI): 323.97 ($C_{17}H_{12}FN_4O_2$, $[M+H]^+$). Anal.Calcd for $C_{17}H_{11}FN_4O_2$: C, 63.35; H, 3.44; N, 17.38%. Found: C, 63.38; H, 3.45; N, 17.37%.

4.2.3.18. 2-(3-Methoxyphenyl)-5-((quinazolin-4-yloxy)methyl)-1,3,4-oxadiazole (4r)

Yield: 48%; m.p. 116-117 □. ^{1}H NMR(400 MHz, DMSO): 3.80(s, 3H), 5.54(s, 2H), 7.18(m, 1H), 7.51(m, 4H), 7.71(d, *J*=8.00 Hz, 1H), 7.86(m, 1H), 8.13(m, 1H), 8.54(s, 1H). ^{13}C NMR (101 MHz, DMSO) δ: 164.55, 163.37, 160.47, 148.29, 135.35, 129.69, 128.00(2), 127.65(2), 126.46, 121.87, 121.69, 119.86, 115.17, 1121.36, 55.39, 41.17. MS (ESI): 335.63 ($C_{18}H_{15}N_4O_3$, $[M+H]^+$). Anal.Calcd for $C_{18}H_{14}N_4O_3$: C, 64.66; H, 4.22; N, 16.76%. Found: C, 64.68; H, 4.25; N, 16.73%.

4.2.3.19. 2-(4-Chlorophenyl)-5-((quinazolin-4-yloxy)methyl)-1,3,4-oxadiazole (4s)

Yield: 43%; m.p. 101-103 □. ^{1}H NMR(400 MHz, DMSO): 5.54(s, 1H), 7.56(m, 1H), 7.63(d, *J*=8.64Hz, 2H), 7.71(d, *J*=7.84 Hz, 1H), 7.85(m, 1H), 7.94(d, *J*=8.64, 2H), 8.13(m, 1H), 8.53(s, 1H). ^{13}C NMR (101 MHz, DMSO) δ: 163.85, 163.37, 160.45, 148.33, 148.14, 135.35, 130.67, 129.75(2), 128.35(2), 127.87, 126.62, 124.32, 121.83, 117.24, 41.17. MS (ESI): 339.25 ($C_{17}H_{12}ClN_4O_2$, $[M+H]^+$). Anal.Calcd for $C_{17}H_{11}ClN_4O_2$: C, 60.08; H, 3.27; N, 16.54%. Found: C, 60.06; H, 3.26; N, 16.57%.

4.2.3.20. 2-(4-Bromophenyl)-5-((quinazolin-4-yloxy)methyl)-1,3,4-oxadiazole (4t)

Yield: 52%; m.p. 134-135 □. ^{1}H NMR(400 MHz, DMSO): 5.54(s, 2H), 7.56(t, *J*=7.08 Hz, 1H), 7.70(m, 1H), 7.78(m, 2H), 7.87(m, 3H), 8.13(m, 1H), 8.53(s, 1H). ^{13}C NMR (101 MHz, DMSO) δ: 164.28, 163.21, 160.46, 148.30, 148.13, 135.35, 132.18, 131.76, 128.00(2), 127.88(2), 126.62, 126.28, 122.71, 121.82, 41.15. MS (ESI): 384.39 ($C_{17}H_{12}BrN_4O_2$, $[M+H]^+$). Anal.Calcd for $C_{17}H_{11}BrN_4O_2$: C, 53.28; H, 2.89; N, 14.62%. Found: C, 53.30; H, 2.90; N, 14.60%.

4.2.3.21. 2-Phenyl-5-((quinazolin-4-yloxy)methyl)-1,3,4-oxadiazole (4u)

Yield: 49%; m.p. 112-113 □. ^{1}H NMR(400 MHz, DMSO): 5.54(s, 2H), 7.57(m, 4H), 7.70(d, *J*=7.92 Hz, 1H), 7.85(m, 1H), 7.93(m, 2H), 8.12(m, 1H), 8.53(s, 1H). ^{13}C NMR (101 MHz, DMSO) δ: 164.90, 163.03, 160.47, 148.32, 148.15, 135.35, 132.65, 129.98(2), 128.00, 127.89(2), 127.03, 126.62, 123.50, 121.83, 41.19. MS (ESI): 305.87 ($C_{17}H_{13}N_4O_2$, $[M+H]^+$). Anal.Calcd for $C_{17}H_{12}N_4O_2$: C, 67.10; H, 3.97; N, 18.41%. Found: C, 67.11; H, 3.99; N, 18.38%.

4.2.3.22. 2-(4-Nitrophenyl)-5-((quinazolin-4-yloxy)methyl)-1,3,4-oxadiazole (4v)

Yield: 37%; m.p. 167-168 □. ^{1}H NMR(400 MHz, DMSO): 5.63(s, 2H), 7.59(m, 1H), 7.74(d, *J*=7.80 Hz, 1H), 7.88(m, 1H), 8.16(m, 1H), 8.22(m, 2H), 8.40(m, 2H), 8.58(s, 1H). ^{13}C NMR (101 MHz, DMSO) δ: 164.85, 163.33, 160.47, 148.32, 148.15, 135.35, 132.25, 128.00(2), 127.88(2), 126.62, 123.50, 121.83, 117.18, 41.17. MS (ESI): 350.90 ($C_{17}H_{12}N_5O_4$, $[M+H]^+$). Anal.Calcd for $C_{17}H_{11}N_5O_4$: C, 58.45; H, 3.17; N, 20.05%. Found: C, 58.44; H, 3.19; N, 20.02%.

4.3. Antiproliferation assay

The antiproliferative activity of the prepared compounds **4a-4v** against A549, MCF-7 and Hela was evaluated as described in the literature with some modifications.[33] Target tumor cells were grown to log phase in DMEM medium supplemented with 10% fetal bovine serum. After reaching a dilution of 3 x 10^4 cells mL^{-1} with the medium, 100 μL of the obtained cell suspension was added to each well of 96-well culture plates. Subsequently, incubation was performed at 37 □ in 5% CO_2 atmosphere for 24 h before the cytotoxicity assessment. Tested samples at pre-set concentrations were added to wells with tivozanib being employed as a positive reference. After 24 h exposure period, 10 μL of PBS containing 5 *m*g/mL of MTT was added to each well. After 4 h, the medium was replaced by 150 μL DMSO to dissolve the purple formazan crystals produced. The plates were read on a Victor-V multilabel counter (Perkin-Elmer) using the default europium detection protocol. Percent

inhibition or IC_{50} values of compounds were calculated by comparison with DMSO treated control wells. The results are shown in Table 2.

4.4. Kinase assay

The full-length coding sequence of human KDR/GST fusion protein was constructed from the human KDR (NP_002244) (Asp807-Val1356) and the N-terminal polyhistidinetagged GST tag. The fusion protein consist of 787 amino acids and has the molecular weight of 89.3 kDa. The VEGFR 2 kinase assay was performed as the method mentioned in literature.[22]

96-well plates were coated at room temperature for 1-2 h with 100 μL per well of 25 μg/mL poly-(Glu_4-Tyr) peptide (Sigma) in Tris-buffered saline (TBS) (25 *m*M Tris, pH 7.2, 150 *m*M NaCl). Unbound peptide was washed three times with PBS. The cytoplasmic domain of VEGFR2, PDGFR, EGFR, bFGF enzyme were diluted (depending on the specific activity of the batch, from 10- to 20- fold) in 0.1% BSA/4 *m*M HEPES. A master mix of enzyme plus kinase buffer was prepared: (per well) 10 μL of diluted enzyme, 10 μL of kinase buffer (4 *m*M HEPES, pH 7.4, 1.25 *m*M $MnCl_2$, 20 *m*M Na_3VO_4) and compounds (10 μL) prepared in 100% dimethyl sulfoxide (DMSO) were added to wells with appropriate density. Controls were done by adding DMSO alone, i.e., no test compound, to wells containing the master mix of enzyme plus kinase buffer. After 15 min at room temperature, ATP/$MgCl_2$ (20 μL of 25 μM ATP, 25 *m*M $MgCl_2$, 10 *m*M HEPES, pH 7.4) was added to each well to initiate the reaction. Final concentrations of the assay components were 10 μM ATP, 10 *m*M $MgCl_2$, 1 *m*M $MnCl_2$, 4 *m*M HEPES, pH 7.4, 20 μM Na_3VO_4, 20 μg/mL BSA. After 40 min at room temperature, the liquid was removed, and plates were washed three times with PBST (PBS with 0.05% Tween-20). The wells were then incubated for 1 h at room temperature with 75 μL of 0.1 μg/mL europium-conjugated anti-phosphotyrosine antibody (PT66; Perkin-Elmer) prepared in the assay buffer (Perkin- Elmer). Plates were washed three times with PBST and then incubated for 15 min in the dark with 100 μL of enhancement solution (Perkin-Elmer). Plates were read in a Victor-V multilabel counter (Perkin-Elmer) using the default europium

detection protocol. Percent inhibition or IC_{50} values of compounds were calculated by comparison with DMSO-treated control wells.

4.6. Docking simulations

Molecular docking of compound **4j** into the three dimensional X-ray structure of human VEGFR (PDB code: 4ASE) was carried out using the Discovery Studio (version 3.5) as implemented through the graphical user interface DS-CDOCKER protocol. DS-CDOKER is a molecular docking program based on CHARMM. The crystal structures of the protein complex were retrieved from the RCSB Protein Data Bank (http://www.rcsb.org/pdb/home/home.do). All synthesized compounds were full minimized to prepare suitable ligands structure. The crystal structure was optimized after taking the original ligand and all bound waters out, adding hydrogen. Molecular docking of all synthesized compounds was then carried out through the Discovery Studio.[34]

Acknowledgement

This work was supported by the Jiangsu National Science Foundation (no. BK2009239) and the Fundamental Research Fund for the Central Universities (no. 1092020804).

References and notes

1. A. Farce, C. Loge, S. Gallet, N. Lebegue, P. Carato, P. Chavatte, P. Berthelot and D. Lesieur, *J. Enzym. Inhib. Med. Ch.*, 2004, 19, 541.
2. P. Anand, A. B. Kunnumakara, C. Sundaram, K. B. Harikumar, S. T. Tharakan, O. S. Lai, B. Sung and B. B. Aggarwal, *Pharm. Res.*, 2008, 25, 2097.
3. K. Sikora, S. Advani, V. Koroltchouk, I. Magrath, L. Levy, H. Pinedo, G. Schwartsmann, M. Tattersall and S. Yan, *Ann. Oncol.*, 1999, 10, 385.
4. R. Pérez-Tomás, *Curr. Med. Chem.*, 2006, 13, 1859.
5. J. Bange, E. Zwick and A. Ullrich, *Nat. Med.*, 2001, 7, 548.
6. P. M. Hoff and K. K. Machado, *Cancer. Treat. Rev.*, 2012, 38, 825.

7. R. J. DeBerardinis, J. J. Lum, G. Hatzivassiliou and C. B. Thompson, *Cell metabolism*, 2008, 7, 11.
8. N. Ferrara, K. J. Hillan and W. Novotny, *Biochem. Bioph. Res. Co.*, 2005, 333, 328.
9. N. Ferrara, H. Gerber and J. LeCouter, *Nat. Med.*, 2003, 9, 669.
10. K. Holmes, O. L. Roberts, A. M. Thomas and M. J. Cross, *Cell. Signal.*, 2007, 19, 2003.
11. K. Sina, T. Sonia, L. Xiujuan, G. Laura and C. Lena, *Biochem. J.*, 2011, 437, 169.
12. F. Musumeci, M. Radi, C. Brullo and S. Schenone, *J. Med. Chem.*, 2012, 55, 10797.
13. G. Klement, P. Huang, B. Mayer, S. K. Green, S. Man, P. Bohlen, D. Hicklin and R. S. Kerbel, *Clin. Cancer. Res.*, 2002, 8, 221.
14. R. M. Bremnes, C. Camps and R. Sirera, *Lung. Cancer-J. Iaslc.*, 2006, 51, 143.
15. O. Gallo, A. Franchi, L. Magnelli, I. Sardi, A. Vannacci, V. Boddit, V. Chiarugi and E. Masini, *Neoplasia*, 2001, 3, 53.
16. Y. Zhang, F. Guessous, A. Kofman, D. Schiff and R. Abounader, *IDrugs*, 2010, 13, 112.
17. L. M. Ellis and D. J. Hicklin, *Nat. Rev. Cancer.*, 2008, 8, 579.
18. P. Martin, S. Oliver, S. Kennedy, E. Partridge, M. Hutchison, D. Clarke and P. Giles, *Clin. Ther.*, 2012, 34, 221.
19. D. Strumberg, *Drugs. Today. (Barc).*, 2005, 41, 773.
20. M. McTigue, B. W. Murray, J. H. Chen, Y. Deng, J. Solowiej and R. S. Kania, *Proceedings of the National Academy of Sciences*, 2012, 109, 18281.
21. S. R. Wedge, D. J. Ogilvie, M. Dukes, J. Kendrew, R. Chester, J. A. Jackson, S. J. Boffey, P. J. Valentine, J. O. Curwen and H. L. Musgrove, *Cancer. Res.*, 2002, 62, 4645.
22. J. Sun, D. Li, J. Li, F. Fang, Q. Du, Y. Qian and H. Zhu, *Organic & biomolecular chemistry*, 2013, 11, 7676.
23. J. Stamos, M. X. Sliwkowski and C. Eigenbrot, *J. Biol. Chem.*, 2002, 277, 46265.
24. A. Wissner, M. B. Floyd, B. D. Johnson, H. Fraser, C. Ingalls, T. Nittoli, R. G. Dushin, C. Discafani, R. Nilakantan and J. Marini, *J. Med. Chem.*, 2005, 48, 7560.
25. C. Chen, B. Song, S. Yang, G. Xu, P. S. Bhadury, L. Jin, D. Hu, Q. Li, F. Liu and W.

Xue, *Bioorgan. Med. Chem.*, 2007, 15, 3981.

26. A. Zarghi, S. A. Tabatabai, M. Faizi, A. Ahadian, P. Navabi, V. Zanganeh and A. Shafiee, *Bioorg. Med. Chem. Lett.*, 2005, 15, 1863.
27. D. Dewangan, A. Pandey, T. Sivakumar, R. Rajavel and R. D. Dubey, *Int. J. Chem. Tech. Res.*, 2010, 2, 1397.
28. K. S. Bhat, M. S. Karthikeyan, B. S. Holla and N. S. Shetty, *Indian. J. Chem. B*, 2004, 43, 1765.
29. C. R. W. Guimarães, D. L. Boger and W. L. Jorgensen, *J. Am. Chem. Soc.*, 2005, 127, 17377.
30. V. P. Rahman, S. Mukhtar, W. H. Ansari and G. Lemiere, *Eur. J. Med. Chem.*, 2005, 40, 173.
31. J. Mirzaei, M. Amini, H. Pirelahi and A. SHAFLEE, *J. Heterocyclic. Chem.*, 2008, 45, 921.
32. <http://www.rcsb.org/pdb/explore/explore.do?structureId=4ASE/>
33. X. Chen, C. Plasencia, Y. Hou and N. Neamati, *J. Med. Chem.*, 2005, 48, 1098.
34. G. Wu, D. H. Robertson, C. L. Brooks and M. Vieth, *J. Comput. Chem.*, 2003, 24, 1549-1562.

Figure Captions

Table 1. Structure of compounds **4a-4v**.

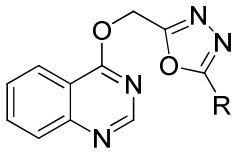

compound	R	compound	R	compound	R
4a	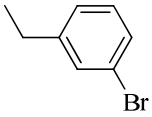	**4i**	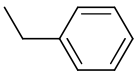	**4q**	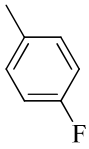
4b	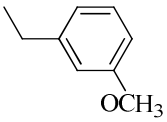	**4j**	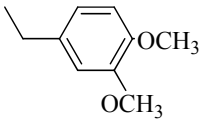	**4r**	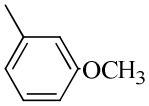
4c	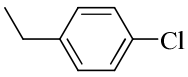	**4k**	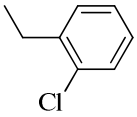	**4s**	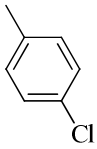
4d	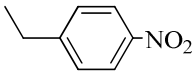	**4l**	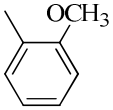	**4t**	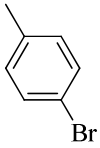
4e	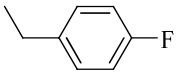	**4m**	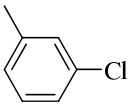	**4u**	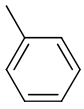
4f	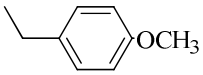	**4n**	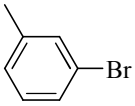	**4v**	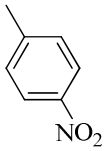
4g	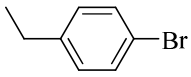	**4o**	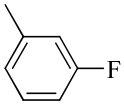		
4h	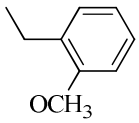	**4p**	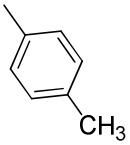		

Table 2. Inhibition of cancer cells proliferation by compounds **4a-4v**.

Compounds	$IC_{50} \pm SD(\mu M)$		
	MCF-7[a]	A549[b]	Hela[c]
4a	2.05 ± 0.07	1.51 ± 0.04	2.16 ± 0.07
4b	0.87 ± 0.06	0.96 ± 0.03	0.87 ± 0.03
4c	2.55 ± 0.16	2.06 ± 0.09	2.73 ± 0.16
4d	0.67 ± 0.07	0.94 ± 0.04	0.84 ± 0.02
4e	4.59 ± 0.24	5.49 ± 0.36	4.65 ± 0.19
4f	0.77 ± 0.04	0.87 ± 0.05	0.79 ± 0.03
4g	1.89 ± 0.02	0.86 ± 0.03	1.51 ± 0.08
4h	2.54 ± 0.08	1.87 ± 0.02	1.75 ± 0.06
4i	16.23 ± 0.67	14.96 ± 0.97	14.21 ± 0.71
4j	0.23 ± 0.04	0.32 ± 0.02	0.38 ± 0.03
4k	4.63 ± 0.26	5.25 ± 0.23	4.92 ± 0.14
4l	7.36 ± 0.12	8.96 ± 0.16	8.65 ± 0.18
4m	7.19 ± 1.64	8.07 ± 0.89	8.67 ± 0.85
4n	9.58 ± 0.57	8.27 ± 0.85	9.98 ± 1.36
4o	> 50	44.32 ± 0.07	48.31 ± 1.46
4p	18.73 ± 1.69	17.52 ± 1.47	17.47 ± 1.36
4q	22.94 ± 1.12	19.39 ± 1.86	17.7 ± 1.83
4r	7.3 ± 1.04	6.32 ± 0.75	7.43 ± 0.77
4s	13.12 ± 0.63	13.17 ± 0.36	15.44 ± 0.27
4t	8.94 ± 0.22	8.38 ± 0.63	8.35 ± 0.69
4u	34.2 ± 1.57	32.87 ± 1.19	35.07 ± 1.23
4v	16.1 ± 1.25	19.35 ± 0.83	16.35 ± 1.49
tivozanib	0.38 ± 0.060	0.62 ± 0.030	0.34 ± 0.020

[a] Inhibition of the growth of MCF-7 cell lines.

[b] Inhibition of the growth of A549 cell lines.

[c] Inhibition of the growth of Hela cell lines.

Table 3. Inhibition of selected kinases IC_{50} [a] (*nM*)

Compounds	VEGFR2	EGFR	bFGF	PDGFR
4a	12.31	310.58	164.49	73.52
4b	5.83	302.79	152.33	66.13
4c	19.05	335.96	182.17	82.06
4d	4.73	293.57	136.32	55.33
4e	33.25	357.76	201.25	100.16
4f	5.28	295.51	146.76	63.69
4g	11.43	305.20	154.23	70.75
4h	15.07	332.58	179.06	80.49
4i	55.16	510.72	490.12	273.39
4j	2.32	216.43	98.55	39.64
4k	36.31	363.04	232.39	102.64
4l	29.50	320.89	194.86	90.76
4m	40.53	394.81	216.44	116.14
4n	43.65	462.27	386.21	152.08
4o	98.75	587.42	685.01	325.12
4p	60.38	507.76	517.94	334.11
4q	67.08	496.61	561.69	287.52
4r	41.13	414.37	213.52	140.73
4s	43.08	476.68	421.19	162.58
4t	50.14	453.56	338.62	185.28
4u	78.81	548.06	624.84	296.41
4v	59.44	493.23	516.52	241.78
tivozanib	3.40	116.64	108.15	45.93

[a] IC_{50} values were averaged values determined by at least two independent experiments. Variation was generally 5%.

Table 4. The docking calculation of the synthesized compounds (**4a-4v**)

Compounds	CDOKER INTERATION ENERGY kcal/mol	Compounds	CDOKER INTERATION ENERGY kcal/mol
4a	-47.2314	**4l**	-45.6047
4b	-48.9269	**4m**	-43.7809
4c	-46.4385	**4n**	-43.4841
4d	-47.7327	**4o**	-39.4104
4e	-44.6077	**4p**	-42.3049
4f	-47.0279	**4q**	-42.2217
4g	-47.4352	**4r**	-43.904
4h	-47.1029	**4s**	-42.9932
4i	-42.8375	**4t**	-43.55
4j	-50.5831	**4u**	-41.4659
4k	-45.1589	**4v**	-42.4093
Tivozanib	-47.6633		

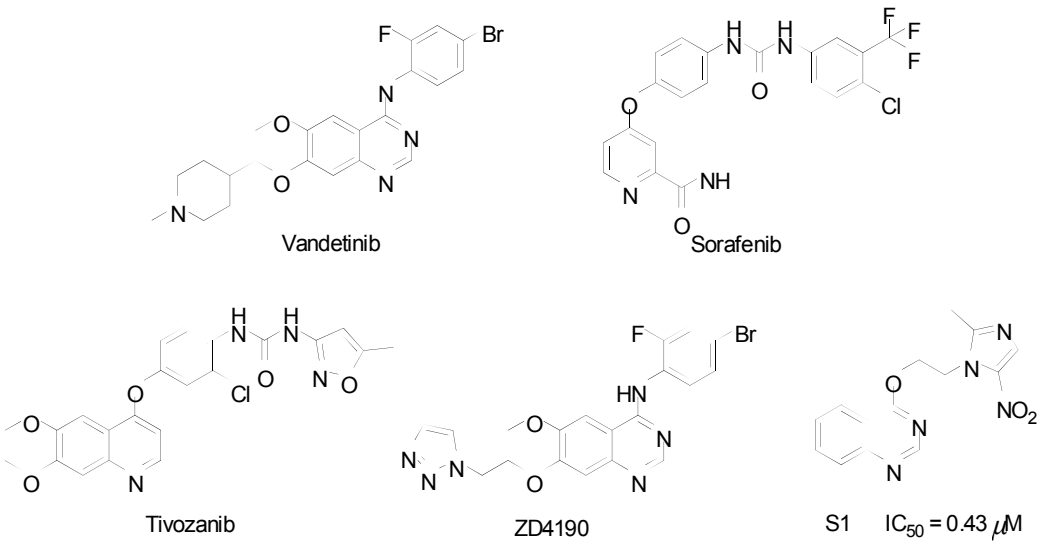

Figure 1. Various VEGFR tyrosine kinase inhibitors

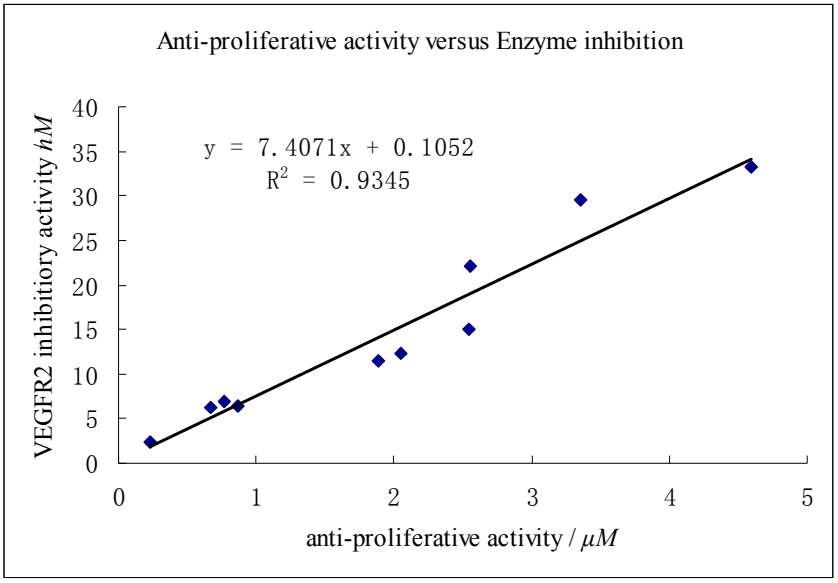

Figure 2. Correlation between the anti-proliferative activity against MCF-7 and the VEGFR2 inhibitory activity, $R^2 = 0.9345$, which indicated that there was a moderate correlation between VEGFR2 inhibition and inhibition of cellular proliferation

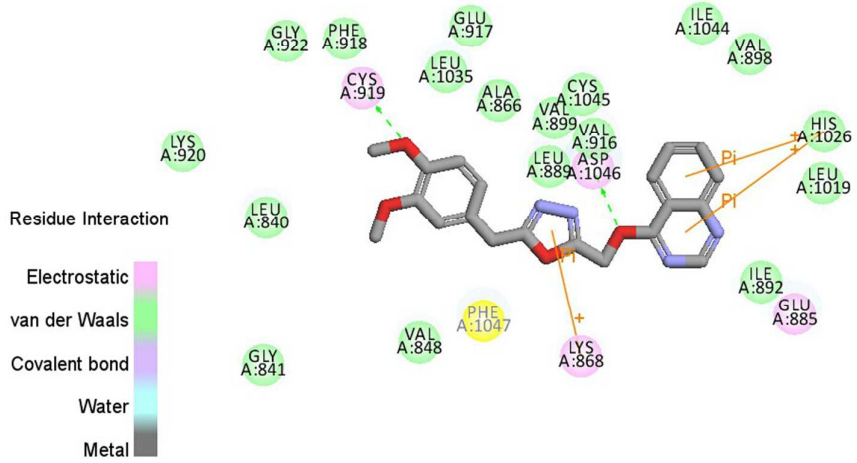

Figure 3. 2D molecular docking model of compound **4j** with VEGFR2 (entry 4ASE in the Protein Data Bank).

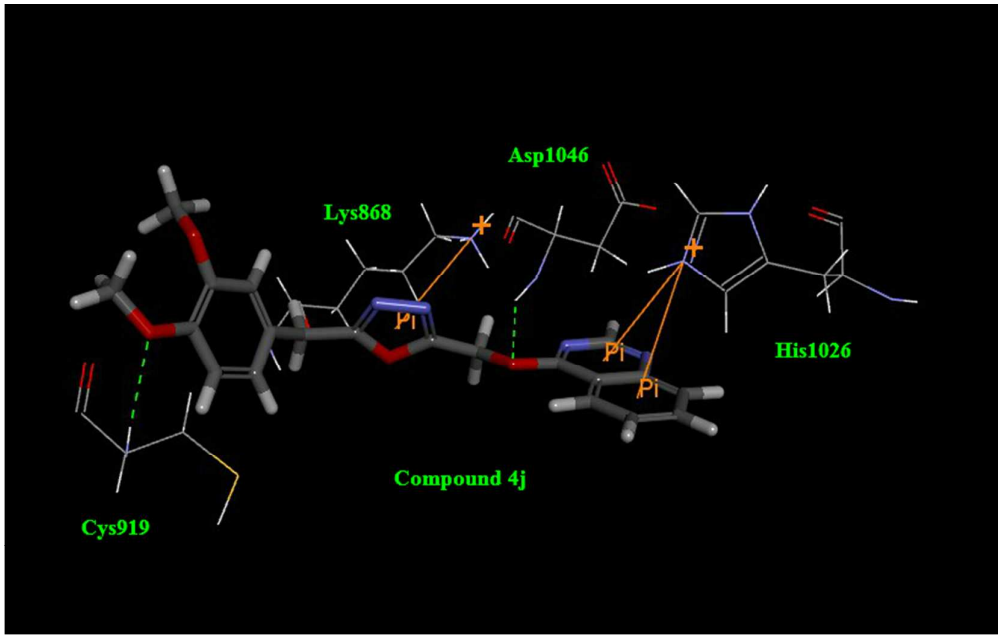

Figure 4. 3D molecular docking model of compound **4j** with VEGFR2 (entry 4ASE in the Protein Data Bank).

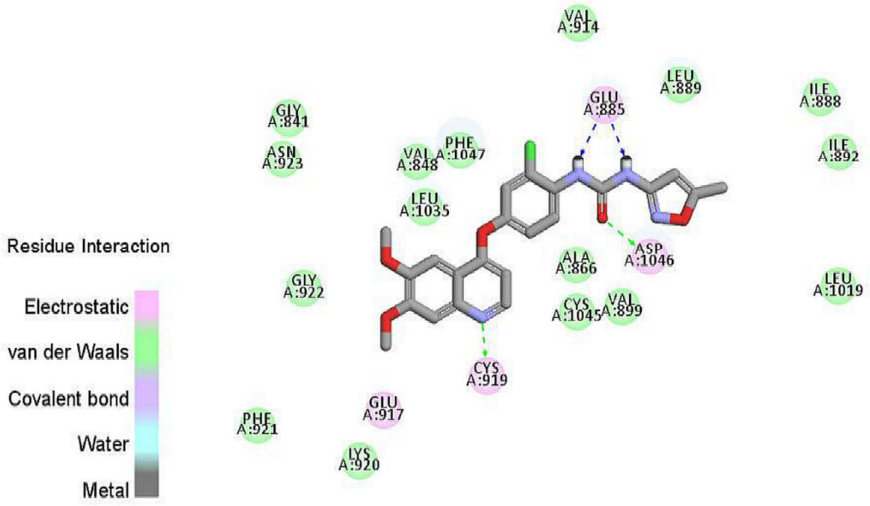

Figure 5. 2D molecular docking model of tivozanib with VEGFR2 (entry 4ASE in the Protein Data Bank).

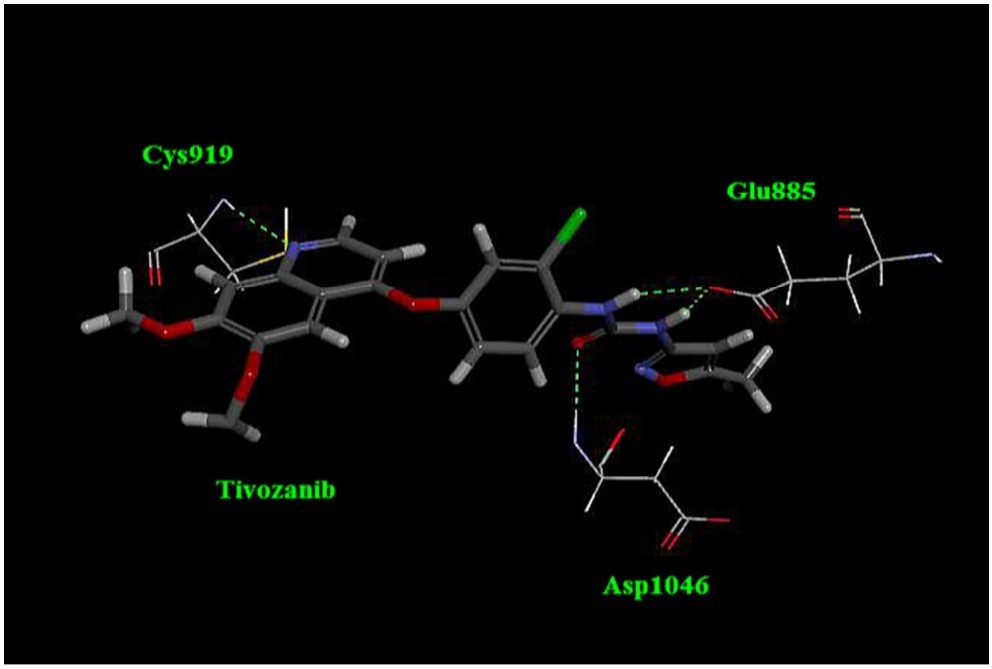

Figure 6. 3D molecular docking model of tivozanib with VEGFR2 (entry 4ASE in the Protein Data Bank).

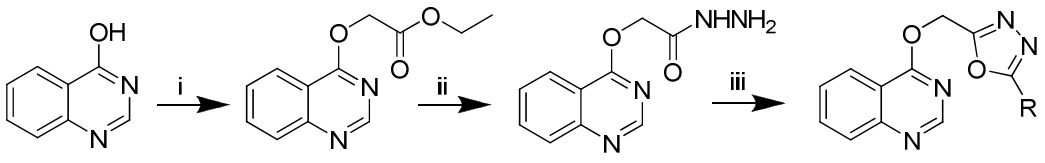

1 **2** **3** **4a-4v**

Scheme 1. Synthesis of compounds **4a-4v**. Reagents and conditions: (i) ethyl-bromacetate, Cs_2CO_3, DMF /reflux/24 h; (ii) hydrazine hydrate, methanol /0 □/4.5 h; (iii) substituted carboxylic acids, phosphoryl chloride/reflux/10-16h.